

Article

# An Assessment of the Mechanical Properties and Microstructural Analysis of Dissimilar Material Welded Joint between Alloy 617 and 12Cr Steel

Hafiz Waqar Ahmad \*, Jeong Ho Hwang, Ju Hwa Lee and Dong Ho Bae \*

Graduate School of Mechanical Engineering, Sungkyunkwan University, Suwon 440-746, Korea; reflika@skku.edu (J.H.H.); juhwa0207@skku.edu (J.H.L.)

\* Correspondence: waqar543@skku.edu (H.W.A.); bae@yurim.skku.ac.kr (D.H.B.); Tel.: +82-31-290-7443 (D.H.B.)

Academic Editor: Giuseppe Casalino

Received: 29 August 2016; Accepted: 10 October 2016; Published: 14 October 2016

**Abstract:** The most effective method to reduce CO<sub>2</sub> gas emission from the steam power plant is to improve its performance by elevating the steam temperature to more than 700 °C. For this, it is necessary to develop applicable materials at high temperatures. Ni-based Alloy 617 and 12Cr steel are used in steam power plants, due to their remarkable mechanical properties, high corrosion resistance, and creep strength. However, since Alloy 617 and 12Cr steel have different chemical compositions and thermal and mechanical properties, it is necessary to develop dissimilar material welding technologies. Moreover, in order to guarantee the reliability of dissimilar material welded structures, the assessment of mechanical and metallurgical properties, fatigue strength, fracture mechanical analysis, and welding residual stress analysis should be conducted on dissimilar material welded joints. In this study, first, multi-pass dissimilar material welding between Alloy 617 and 12Cr steel was performed under optimum welding conditions. Next, mechanical properties were assessed, including the static tensile strength, hardness distribution, and microstructural analysis of a dissimilar material welded joint. The results indicated that the yield strength and tensile strength of the dissimilar metal welded joint were higher than those of the Alloy 617 base metal, and lower than those of the 12Cr steel base metal. The hardness distribution of the 12Cr steel side was higher than that of Alloy 617 and the dissimilar material weld metal zone. It was observed that the microstructure of Alloy 617 HAZ was irregular austenite grain, while that of 12Cr steel HAZ was collapsed martensite grain, due to repeatable heat input during multi-pass welding.

**Keywords:** dissimilar material welding; Ni-based Alloy 617; 12Cr steel; mechanical properties; microstructural characterization

## 1. Introduction

Environmental pollution from energy generation is a topical issue worldwide. There are four ways to improve this problem: the first is to generate energy from renewable energy resources, the second is to use nuclear energy, the third is to use carbon capture and storage before pollutants are released to the atmosphere, and the fourth is to increase energy efficiency by using A-USC (advanced-ultra super critical) thermal power plants that are capable of generating energy at temperatures above 700 °C [1]. A-USC thermal power plants have improved thermal efficiency, and reduced CO<sub>2</sub> emissions [2,3]. However, at this elevated temperature, it is very difficult to find applicable materials that can withstand extreme environments. Ni-based super alloys and high chromium steel are suitable candidates for such extreme environments in the power generation industry due to their exceptional metallurgical stability at high temperatures, and excellent mechanical properties, such as high creep rupture strength, and good oxidation and corrosion resistance [4,5].

Alloy 617 is a nickel-chromium-cobalt-molybdenum based alloy that is most commonly used in gas turbines for combustion cans and ducts, as well as for industrial furnace components and applications. Alloy 617 is primarily known for its remarkable metallurgical stability [6]. It brings a wide variety of other outstanding properties, e.g., high temperature oxidation resistance due to added aluminum, and solid solution strengthening due to cobalt and molybdenum content [7]. It is easy to fabricate and can be easily joined through conventional welding techniques [8].

12Cr steel with the addition of Mo, Nb, N, W, and other elements possesses improved toughness, good oxidation and corrosion resistance at elevated temperatures, high tensile strength and ductility, and promising creep rupture strength. 12Cr steel is currently used for components in gas turbines, boilers, and steam power plant turbines [9,10].

A typical steam turbine rotor has three major stages: the high temperature and pressure stage, the middle temperature and pressure stage, and the low temperature and pressure stage. Since Ni-based super Alloy 617 is a very difficult material to work on, it is partially applicable to the high and low pressure stages. Use of Ni-based super Alloy 617 in lower pressure stage requires its joining with 12Cr steel, which is currently used in the low pressure stage [11]. In order to guarantee the mechanical reliability of dissimilar material weld between Ni-based Alloy 617 and 12Cr steel, it is necessary to develop welding technology between dissimilar materials and perform welding stress analysis, strength assessment, and the assessment of corrosion characteristics at the dissimilar material weld.

A significant amount of research has been carried out on Ni-based alloys as well as Cr steel alloys in recent decades [4,10,12–15]. However, it is difficult to find a systematic study on the dissimilar material welding and welded joint of Alloy 617 and 12Cr steel. In this work, a dissimilar material welding between Alloy 617 and 12Cr steel was carried out using Direct Current Straight Polarity (DCSP) tungsten inert gas (TIG) welding technology, and an assessment of the mechanical properties and a microstructural analysis of the dissimilar material weld were performed.

## 2. Dissimilar Material Welding between Ni-Based Alloy 617 and 12Cr Steel

### 2.1. Materials and Welding Procedure

In this work, DCSP TIG welding technology was used for the dissimilar material welding process. Tables 1 and 2 illustrate the chemical composition and mechanical properties of Alloy 617, 12Cr steel, and Thyssen 617, which is filler metal of a wire 1 mm in diameter. The welding conditions, such as the electrode shape, arc length, welding wave mode (CW or pulse), and welding heat input, were controlled using a real time monitoring system. The optimum welding conditions were determined by repeatedly performing preliminary welding with a variety of welding conditions at different shield gas composition and flow rates. Optimized dissimilar material welding conditions are summarized in Table 3.

**Table 1.** Chemical compositions of Alloy 617, Thyssen 617, and 12Cr steel.

Base/Filler Metal	Chemical Composition (% Weight)											
	Ni	Cr	Co	Mo	Al	C	Fe	Si	Ti	Cu	Mn	S
Alloy 617	44.3	22	12.5	9.0	1.2	0.07	1.5	0.5	0.3	0.2	0.5	0.008
Thyssen 617	45.7	21.5	11.0	9.0	1.0	0.05	1.0	0.1	1	-	-	-
12Cr	0.43	11.6	-	0.04	-	0.13	Bal.	0.4	-	0.1	0.58	-

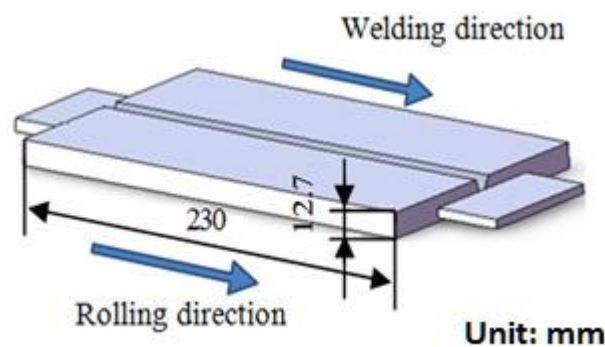
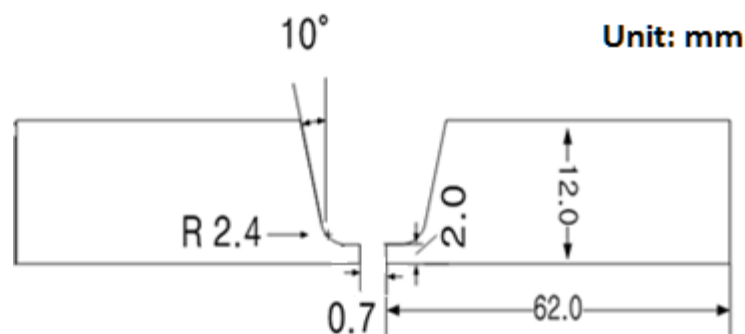
**Table 2.** Mechanical properties of Alloy 617 and 12Cr steel.

Base Material	Y.S. (MPa)	T.S. (MPa)	Elongation	R.A. (%)	M.P. (°C)
Alloy 617	322	732	62	56	1330
12Cr	551	758	18	50	1375

**Table 3.** Multi-pass dissimilar material welding conditions between Alloy 617 and 12Cr steel.

Pass	Shield Gas	Current (A)	Voltage (V)	Welding Speed (cm/min)	Freq. (Hz)
1	Ar-2.5% H <sub>2</sub>	150	10	10	0.5
2	Ar-2.5% H <sub>2</sub>	150	13	10	0.5
3	Ar-2.5% H <sub>2</sub>	150	16	10	0.5
4	Ar-2.5% H <sub>2</sub>	150	16	10	0.5
5	Ar-2.5% H <sub>2</sub>	150	16	10	0.5
6	Ar-2.5% H <sub>2</sub>	150	16	10	0.5
7	Ar-2.5% H <sub>2</sub>	150	16	10	0.5

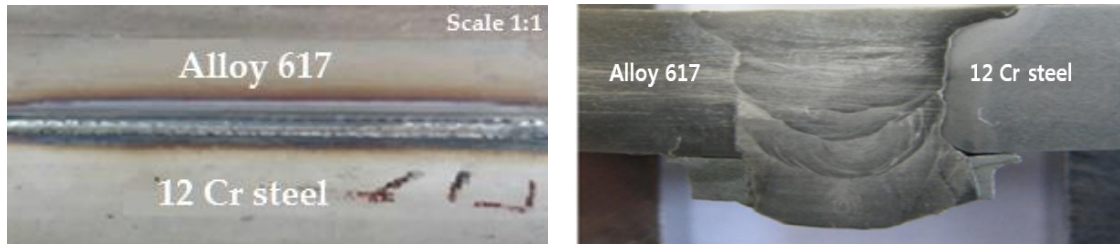
In order to prevent thermal distortion, which is formidably caused by welding heat input during the welding process, both ends of the base metal were fixed with welding jigs. Figure 1 shows that the welding direction was made parallel to the rolling direction of the base metals. The groove shape of Figure 2 was machined in a U-groove to narrow the gap welding [16,17]. Thyssen 617 was used as a filler metal and its chemical composition is shown in Table 1. When welding was completed for each pass, the surface condition of the weld bead was carefully observed, and the welding condition was confirmed. After finishing each pass, for the next pass, the surface of the weld bead was brushed using a copper brush, and the temperature checked was to allow it to cool sufficiently below 70 °C. After welding, the multi-pass welds were inspected by using the ultrasonic testing method.

**Figure 1.** Welding direction for dissimilar material welding between Alloy 617 and 12Cr steel.**Figure 2.** U-groove with narrow gap.

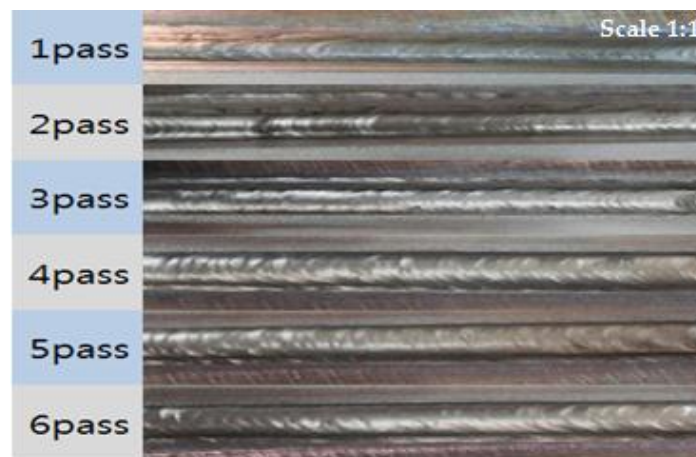
## 2.2. Results of the Dissimilar Welding

Figure 3 shows the top view and cross section of the dissimilar material weld between Alloy 617 plate and the 12Cr steel plate. Figure 4 illustrates the weld bead appearance for each pass. These figures show that there were no weld defects or oxidation phenomenon on the weld surfaces.

Even though it was assumed that out-of-plane thermal distortion would be generated by repeatable welding heat input during the multi-pass welding processes, it was prevented by the constraint of the welding jigs.



**Figure 3.** Dissimilar weld: top view (left) and cross section (right).



**Figure 4.** Weld bead appearance for each pass.

### 3. Assessing Mechanical Properties of Dissimilar Material Welded Joint

#### *Specimen and Procedure*

The specimen dimensions and tensile test procedure, to assess the mechanical properties of dissimilar material welded joint between Alloy 617 and 12Cr steel, was followed as recommended in the ASTM E8M standard [18]. Figure 5 shows that the weld metal, the heat affected zone (HAZ), and both base metals of Alloy 617 and 12Cr steel are included within the range of the gauge length of the specimens. Before assessing the mechanical properties of the dissimilar material welded joint, tensile tests for base metals (Alloy 617 and 12Cr steel) were performed to measure their mechanical properties. Mechanical properties of the base metals and dissimilar material welded joint were assessed using a material testing system (INSTRON 8801, Instron Korea, LLC., Seoul, Korea) as shown in Figure 6 at room temperature. In the tensile test, the loading speed was controlled by the displacement of 1 mm/min.

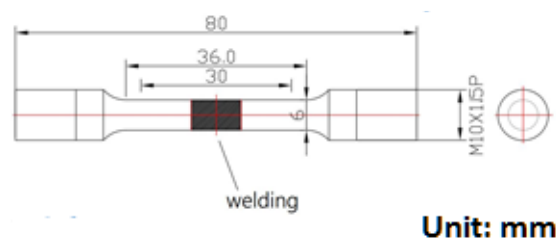


**Figure 5.** Configuration of tensile test specimen (ASTM E8M).



**Figure 6.** Test equipment (10 tons, Instron 8801).

The hardness distribution on the section, including base metal, HAZ, and the weld metal of dissimilar material welded joint, were measured to analyze the effect of multi-pass dissimilar material welding on metallurgical hardness change. Figure 7 shows that hardness tests were performed to compare the hardness distribution for the three positions: top, middle, and bottom of the cross section. The hydraulic micro Vickers hardness tester (Mitutoyo MVK-H2, Mitutoyo Korea Corporation, Gunpo, Korea) was used as hardness test equipment. Hardness distribution of the multi-pass dissimilar material welded joint was measured at a 200 g press-fit load for 5 s.

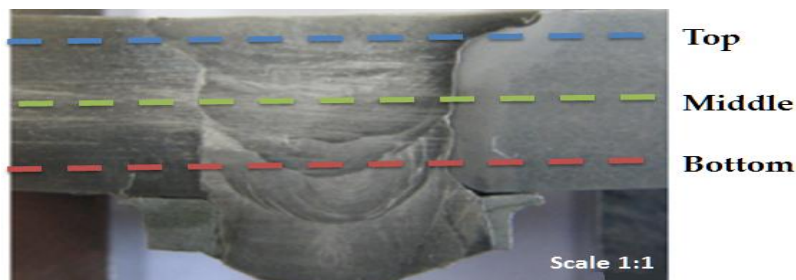


**Figure 7.** Three positions across the cross section of dissimilar material welded joint for hardness distribution measurements.

Optical microscopic observation, using Olympus PME 3 (Olympus Korea Co. LTD., Seoul, Korea), was carried out in order to analyze the microstructure of the dissimilar material welded joint between Alloy 617 and 12Cr steel. Specimen was fabricated from the cross section of the dissimilar material welded joint. In order to analyze the microstructures of dissimilar material welded plate, five position—(a) Alloy 617 base metal; (b) Alloy 617 HAZ; (c) weld metal; (d) 12Cr steel HAZ; and (e) 12Cr steel base metal—were optically observed as shown in Figure 8. Before analyzing the microstructures, the surface of specimen was etched according to ASTM E407 [19]. Three positions—(a), (b), and (c)—were etched for 20 s by using etchant 88 (10 mL of HCl + 20 mL of HNO<sub>3</sub> + 30 mL of distilled water). The other positions—(d) and (e)—were etched for 10 s by using etchant 91 (5 mL of HCl + 5 mL of HNO<sub>3</sub> + 1 g pf picric acid + 200 mL of ethanol). In addition, composition analysis for the five positions of the dissimilar welded joint was performed using energy dispersive X-ray spectroscopy (EDS, EDAX Inc., Mahwah, NJ, USA).

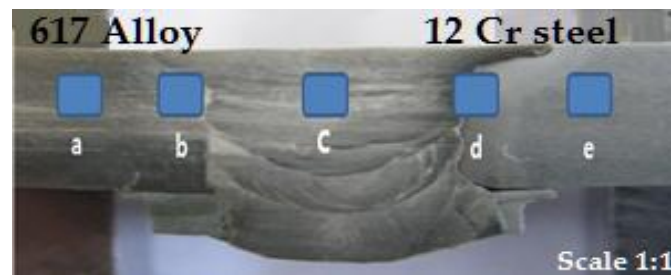


**Figure 8.** Positions of microstructure analysis for the dissimilar material welded joint.

## 4. Results and Discussion

### 4.1. Tensile Test Results

Figure 9a compares the tensile test results of the base metals and the dissimilar material welded joint between Alloy 617 and 12Cr steel. The magnitudes of yield and tensile strength of the dissimilar material welded joint were assessed as 490 MPa and 767 MPa, respectively. These magnitudes are higher than Alloy 617, which has a 443 MPa yield strength and a 675 MPa ultimate tensile strength, and lower than 12Cr steel, which has a 700 MPa and 817 MPa yield and tensile strength, respectively. Failure of dissimilar welded joints occurred mostly at the HAZ of 12Cr steel. Figure 9b shows one of the fractured specimens that has failed at the HAZ of 12Cr steel.

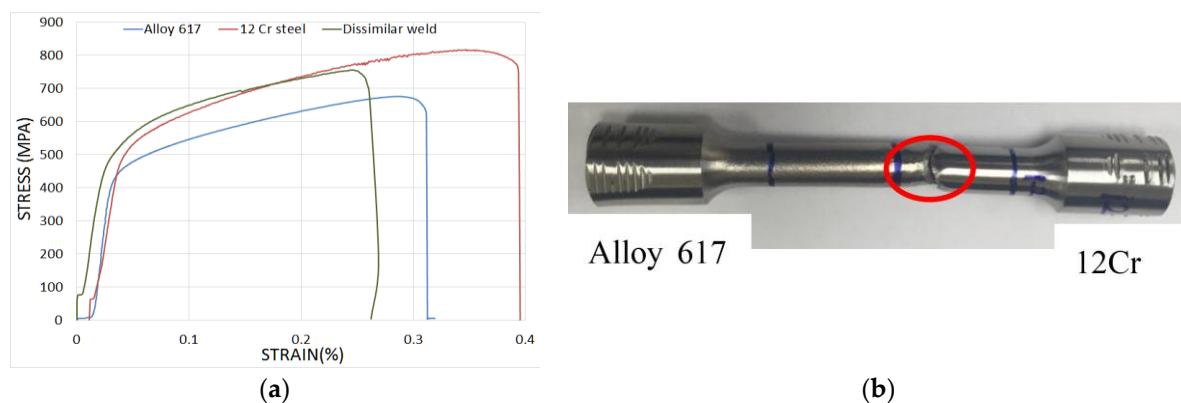


**Figure 9.** (a)  $\sigma$ - $\varepsilon$  curves of dissimilar weld; (b) dissimilar weld fractured specimen.

Although tensile strength of 12Cr steel is higher than that of Alloy 617, but the failure of the dissimilar material weld occurred at the HAZ of 12Cr steel because the heat input during the dissimilar material welding process introduced sufficient metallurgical changes in 12Cr steel HAZ [20]. On the other hand, Ni-based Alloy 617 experienced lesser metallurgical changes compared with 12Cr steel due to heat input during the dissimilar material welding process. In fact, Ni-based Alloy 617 is primarily known for its remarkable metallurgical stability at high temperatures [6].

### 4.2. Hardness Distribution

Figure 10 compares the hardness distribution on the bottom, middle, and top positions of the cross section of the dissimilar material welded joint between Alloy 617 and 12Cr steel. The hardness distribution at the HAZ of 12Cr steel is higher than that of both the weld metal zone and the Alloy 617 base metal. The magnitude of the peak values were assessed as 460–490 Hv at the HAZ of 12Cr steel, and about 220–260 Hv at both the weld metal and the Alloy 617 base metal. It is notable that the hardness distribution of the weld metal zone and the Alloy 617 base metal is almost similar, and the peak values, too, do not show a major difference at the bottom, middle, or top positions in either

zones. The reason for this behavior is the use of Thyssen 617 as filler material, which has a chemical composition similar to that of Alloy 617, as shown in Table 1. Another important observation is that the hardness distribution is nearly uniform on the right side of Figure 10 (weld zone and Alloy 617 zone), while irregular behavior of the hardness distribution is observed on the left side of the figure (HAZ and base metal of 12Cr steel). This behavior is a result of the fact that the microstructure and metallurgical changes in 12Cr steel and Alloy 617 are significantly different when they are affected by the welding heat input during the multi-pass welding process. In fact, it is known that the mechanical properties of Ni-based Alloy 617 are not sensitively influenced by heat [14,21]. As the bottom side experienced more heat cycles during the welding process, the hardness distribution at the bottom side was higher than the top side across the dissimilar material welded joint.

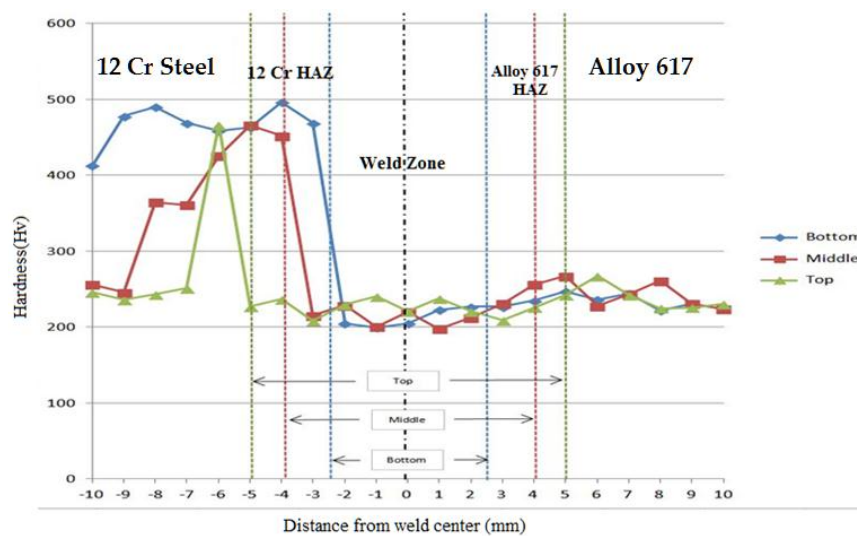


**Figure 10.** Micro hardness profile across the dissimilar metal welded joint.

#### 4.3. Microstructure and Composition Analysis

Figure 11 shows the microstructures of each position of the dissimilar material welded joint. The microstructure of Alloy 617 base metal in Figure 11a shows typical austenite grain. However, HAZ of Alloy 617 in Figure 11b shows irregular austenite grain size from the effect of the welding heat input during the multi-pass welding processes. The microstructure of the weld metal in Figure 11c made by the solidification of fusion metal from the dilution of Alloy 617, Thyssen 617 filler metal, and 12Cr steel, shows dendrite grain. The HAZ of 12Cr steel in Figure 11d shows collapsed martensite grain by the effect of the welding heat input during the multi-pass welding processes, while the microstructure of the 12Cr base metal in Figure 11e shows typical martensite grain.

The composition analysis observed by energy dispersive analysis of X-rays (EDAX) for the five parts of the dissimilar material welded plate is illustrated in Table 4. The effect of the multi-pass welding process of the dissimilar materials is reflected as a slight change in composition of specimen when compared with Table 1. The major composition of the dissimilar metal weld is very similar to the Alloy 617 composition, except for Fe. Table 4 provides information about the composition change at the HAZ and the weld metal.

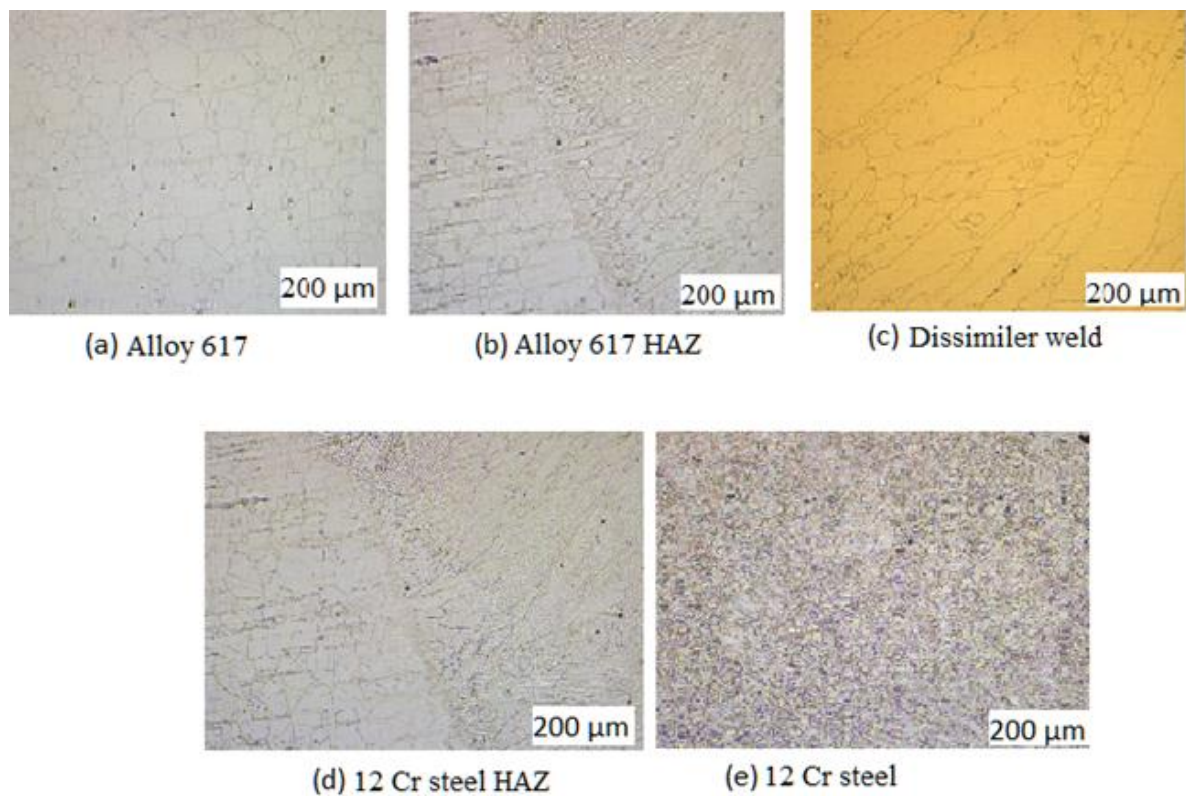


**Figure 11.** Microstructure observation results of dissimilar metal weld: (a) Alloy 617; (b) Alloy 617 HAZ; (c) Dissimilar material weld; (d) 12Cr steel HAZ; (e) 12Cr steel.

**Table 4.** Composition analysis of dissimilar material welded joint (wt. %).

Elements	Alloy 617 Base Metal	Alloy 617 HAZ	Weld Metal	12Cr HAZ	12Cr Base Metal
Mo	10.29	10.70	9.57	-	-
Cr	22.09	21.50	21.11	13.00	10.28
Fe	-	-	12.03	87.00	89.72
Co	13.29	13.76	10.32	-	-
Ni	54.33	54.05	46.97	-	-

Figure 12 shows the fractured tensile test specimen and microscopic observation using a scanning electron microscope (SEM) on the fractured surface of the weld, which occurred on the HAZ of 12Cr steel. As mentioned above, the microstructure of the HAZ of 12Cr steel showed collapsed martensite grain by the effect of welding heat input during the multi-pass welding processes. Additionally, as illustrated in Table 4, the major compositions (Cr and Fe) were slightly changed in the HAZ of 12Cr steel. Even though the microstructure in the HAZ of 12Cr steel shows both collapsed martensite grain and the complicate grain size, as shown in Figure 12b,c, some dimples were observed by the fractography on the fractured surface of the HAZ. Therefore, it was supposed that the failure mode in the HAZ of 12Cr steel was a brittle fracture combined ductile characteristics.

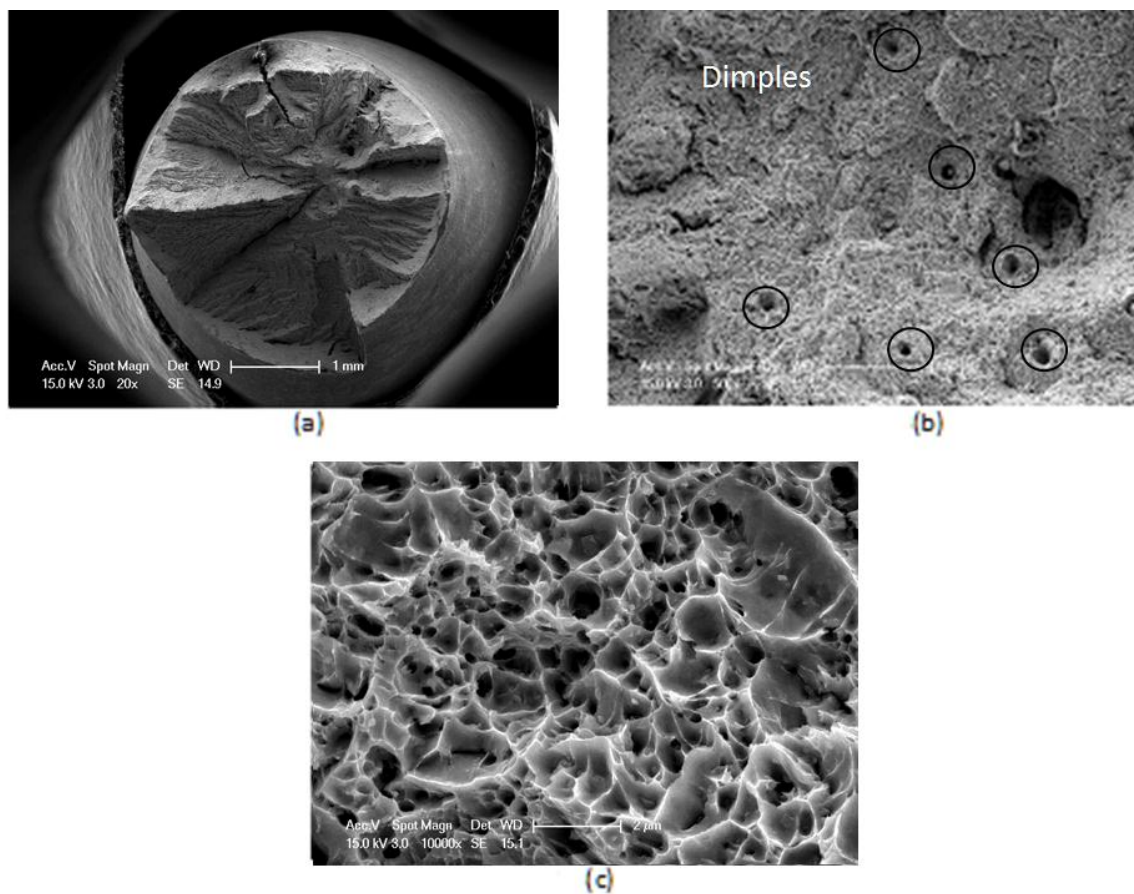


**Figure 12.** Fractography of the dissimilar metal weld at the 12Cr steel side: (a) at 1 mm resolution; (b) at 50  $\mu\text{m}$  resolution; (c) at 2  $\mu\text{m}$  resolution.

## 5. Conclusions

This paper performed and analyzed a dissimilar material welding between Ni-based Alloy 617 and 12Cr steel by DCSP TIG welding technology. In order to guarantee the mechanical reliability of the dissimilar material weld, the mechanical properties, including the tensile strength, the hardness distribution, and changes in microstructure were assessed. The conclusions are as follows:

1. Dissimilar material welding technology using DCSP TIG welding between Ni-based Alloy 617 and 12Cr steel was developed. Optimized major conditions for the DCSP TIG welding were determined as shield gas (Ar-2.5%  $\text{H}_2$  mixed gas), 150 Amp, and 10–16 V.
2. The magnitudes of yield strength and tensile strength of the multi-pass dissimilar material welded joint were assessed as 490 MPa and 767 MPa, respectively. Dissimilar material welded joints mostly failed at the HAZ of 12Cr steel. The mechanical properties of the dissimilar material weld, including yield and tensile strength, were higher than those of the Alloy 617 base metal, and less than those of the 12Cr base metal.
3. The hardness distribution at the HAZ of 12Cr steel is higher than that of the weld metal zone and the Alloy 617 base metal. The magnitudes of the peak values were assessed as 460–490 Hv for the HAZ of 12Cr steel, and about 220–260 Hv for both the weld metal and the Alloy 617 base metal. The hardness distributions for the weld metal zone and Alloy 617 HAZ and the base metal did not show a significant difference.
4. The microstructures of the dissimilar material welded joint, including the Alloy 617 base metal and the HAZ, the weld metal, and the 12Cr steel HAZ and 12Cr base metal, were metallurgically changed via welding heat input during the multi-pass welding process. The microstructures of

Ni-based Alloy 617 base plate and the HAZ of Alloy 617 were analyzed as a typical austenite grain and an irregular austenite grain. However, 12Cr steel HAZ and the 12Cr base metal were analyzed as collapsed martensite and martensite grain, respectively. The microstructure of the weld metal was analyzed as dendrite grain.

**Acknowledgments:** This work was supported by the Reliability Evaluation Lab of the Mechanical Engineering Department, Sungkyunkwan University, Suwon, Korea.

**Author Contributions:** H. Waqar Ahmad conceived and designed the experiments; H. Waqar Ahmad and J.H. Hwang performed the experiments and analyzed the data under the supervision of D.H. Bae; the microstructure analysis was performed in Sungkyunkwan University, Korea; H. Waqar Ahmad wrote the paper.

**Conflicts of Interest:** The authors declare no conflict of interest.

## Abbreviations

The following abbreviations are used in this manuscript:

DMW	Dissimilar Metal Welding
EDAX	Energy Dispersive Analysis of X-rays
HAZ	Heat Affected Zone
DCSP	Direct Current Straight Polarity
TIG	Tungsten Inert Gas

## References

1. Mitigating Climate Change Through Renewables. Available online: <http://www.irena.org/remap/REmap-FactSheet-8-Climate%20Change.pdf> (accessed on 13 October 2016).
2. Weitzel, P.S.; Tanzosh, J.M.; Boring, B. *Advanced Ultra-Supercritical Power Plant (700 to 760C) Design for Indian Coal*; Power Generation Group, Inc.: Barberton, OH, USA, 2012.
3. Higher Efficiency Power Generation Reduces Emissions. Available online: <https://www.scribd.com/document/144610465/Beer-Emissions> (accessed on 13 October 2016).
4. Maile, K. Qualification of Ni-Based Alloys for Advanced Ultra Supercritical Plants. *Proced. Eng.* **2013**, *55*, 214–220. [[CrossRef](#)]
5. Xie, X.; Wu, Y.; Chi, C.; Zhang, M. Superalloys for Advanced Ultra-Super-Critical Fossil Power Plant Application. In *Superalloys*; InTech: Rijeka, Croatia, 2015; pp. 51–76.
6. Development of Materials for Use in A-USC Boilers. Available online: <https://www.mhi.co.jp/technology/review/pdf/e524/e524027.pdf> (accessed on 12 October 2016).
7. Guo, Y.; Wang, B.; Hou, S. Aging Precipitation Behavior and Mechanical Properties of Inconel 617 Superalloy. *Acta Met. Sin.* **2013**, *26*, 307–312. [[CrossRef](#)]
8. Nickel Alloy 617, Inconel® 617. Available online: <http://continentalsteel.com/nickel-alloys/grades/inconel-617/> (accessed on 12 October 2016).
9. Klueh, R.L.; Harries, D.R. Development of High (7%–12%) 2 Chromium Martensitic Steels. In *High-Chromium Ferritic and Martensitic Steels for Nuclear Applications*; ASTM: West Conshohocken, PA, USA, 2001; pp. 5–27.
10. Taban, E.; Kaluc, E.; Atici, T.; Kaplan, E. 9%–12%Cr Steel: Properties and Weldability Aspects, The Situation in Turkish Industry. In *Proceedings of the 2nd International Conference on Welding Technologies and Exhibiton, Ankara, Turkey, 23–25 May 2012*; pp. 203–212.
11. Latest Technologies and Future Prospects for a New Steam Turbine. Available online: <https://www.mhi-global.com/company/technology/review/pdf/e522/e522039.pdf> (accessed on 12 October 2016).
12. Degallaix, G.; Vogt, J.B.; Foct, J. Low Cycle Fatigue of a 12Cr Martensitic Stainless Steel: The Role of Microstructure. In *Low Cycle Fatigue and Elasto-Plastic Behaviour of Materials*; Springer: Dordrecht, The Netherlands, 1987; pp. 95–100.
13. Abe, F. Research and Development of Heat-Resistant Materials for Advanced USC Power Plants with Steam Temperatures of 700 °C and Above. *Engineering* **2015**, *1*, 211–224. [[CrossRef](#)]
14. Mankins, W.L.; Hosier, J.C.; Bassford, T.H. Microstructure and Phase of INCONEL Alloy 617 Stability. *Metall. Trans.* **1974**, *5*, 2579–2590. [[CrossRef](#)]

15. Microstructure and Strength Characteristics of Alloy 617 Welds. Available online: <https://searchworks.stanford.edu/view/11171654> (accessed on 13 October 2016).
16. Corlett, B.J.; Lucas, J.; Smith, J.S. Sensors for Narrow-Gap Welding. *IEEE Proc. A Sci. Meas. Technol.* **1991**, *138*, 213. [[CrossRef](#)]
17. Park, K.D.; Ksmpe, J.Y. A Study on Welding Characteristics of Environment for the Stuctural Inconel. In Proceedings of the KSMPE Conference, Daegu, Korea, November 2004; pp. 216–220.
18. Standard Test Method for Tension Testing of Metallic Materials. Available online: <https://www.astm.org/Standards/E8.htm> (accessed on 12 October 2016).
19. Standard Practice for Micro-Etching Metals and Alloys. Available online: <https://www.scribd.com/document/259609551/ASTM-E407-07-Standard-Practice-for-Microetching-Metals-and-Alloys> (accessed on 12 October 2016).
20. Du Toit, M.; van Rooyen, G.T.; Smith, D. Heat-Affected Zone Sensitization and Stress Corrosion Cracking in 12% Chromium Type 1.4003 Ferritic Stainless Steel. *Corros. Sci.* **2007**, *63*, 395–404. [[CrossRef](#)]
21. Microstructure and Strength Characteristics of Alloy 617 Weld. Available online: <https://inldigitallibrary.inl.gov/sti/3310959.pdf> (accessed on 12 October 2016).



© 2016 by the authors; licensee MDPI, Basel, Switzerland. This article is an open access article distributed under the terms and conditions of the Creative Commons Attribution (CC-BY) license (<http://creativecommons.org/licenses/by/4.0/>).